Acta Crystallographica Section F
Structural Biology and Crystallization Communications
ISSN 1744-3091

Structure of flap endonuclease 1 from the hyperthermophilic archaeon *Desulfurococcus amylolyticus*

Tomoko Mase,[a] Keiko Kubota,[a] Ken-ichi Miyazono,[a] Yutaka Kawarabayasi[b] and Masaru Tanokura[a]*

[a]Department of Applied Biological Chemistry, Graduate School of Agricultural and Life Sciences, The University of Tokyo, 1-1-1 Yayoi, Bunkyo-ku, Tokyo 113-8657, Japan, and [b]National Institute of Advanced Industrial Science and Technology (AIST), 1-1-1 Higashi, Tsukuba, Ibaraki 305-8566, Japan

Correspondence e-mail: amtanok@mail.ecc.u-okyo.ac.jp

Received 20 October 2010
Accepted 17 December 2010

PDB Reference: flap endonuclease 1, 3ory.

Flap endonuclease 1 (FEN1) is a key enzyme in DNA repair and DNA replication. It is a structure-specific nuclease that removes 5′-overhanging flaps and the RNA/DNA primer during maturation of the Okazaki fragment. Homologues of FEN1 exist in a wide range of bacteria, archaea and eukaryotes. In order to further understand the structural basis of the DNA recognition, binding and cleavage mechanism of FEN1, the structure of FEN1 from the hyperthermophilic archaeon *Desulfurococcus amylolyticus* (*Da*FEN1) was determined at 2.00 Å resolution. The overall fold of *Da*FEN1 was similar to those of other archaeal FEN1 proteins; however, the helical clamp and the flexible loop exhibited a putative substrate-binding pocket with a unique conformation.

1. Introduction

Flap endonuclease 1 (FEN1) is an enzyme that is involved in aspects of DNA metabolism such as replication, repair and recombination. It belongs to a structure-specific nuclease family that is evolutionarily conserved from bacteriophages to humans (Harrington & Lieber, 1994; Murante *et al.*, 1995; Hosfield *et al.*, 1998; Hwang *et al.*, 1998). Owing to the importance of FEN1 in genome maintenance, defects in the gene encoding FEN1 give rise to a number of genetic diseases, several ataxias, fragile X syndrome and cancer (Tishkoff *et al.*, 1997; Freudenreich *et al.*, 1998; Schweitzer & Livingston, 1998). FEN1 recognizes 5′-flap structures formed by a branched DNA structure containing a variable length of 5′ single-stranded DNA (Storici *et al.*, 2002; Kaiser *et al.*, 1999; Chapados *et al.*, 2004), one chain of which has an unannealed flapped 5′-end, and removes the flapped DNA strand (Murante *et al.*, 1994). FEN1 plays an important role in the removal of an RNA primer during the maturation of the Okazaki fragment in DNA replication and in the removal of the 5′-flapped DNA structure of damaged nucleotides generated by an incision by an apurinic/apyrimidinic endonuclease. In addition, structural studies of FEN1 proteins have demonstrated the 3′-flap recognition mechanism of FEN1 and the structural basis of the interaction between FEN1 and proliferating cell nuclear antigen (PCNA) in DNA replication (Devos *et al.*, 2007; Hwang *et al.*, 1998; Hosfield *et al.*, 1998; Chapados *et al.*, 2004; Sakurai *et al.*, 2005; Ceska *et al.*, 1996; Mueser *et al.*, 1996; Kim *et al.*, 1995). However, the structural basis of the 5′-flap structure-recognition and cleavage mechanism of FEN1 enzymes remains unclear.

To elucidate this basis, we determined the three-dimensional structure of FEN1 from *Desulfurococcus amylolyticus* (*Da*FEN1), a hyperthermophilic archaeon with an optimum growth temperature range of 363–365 K (Kil *et al.*, 2000), at 2.00 Å resolution using the molecular-replacement method. The overall structure of *Da*FEN1 is similar to those of other FEN1-family proteins, except that *Da*FEN1 has a clamp region with long and stable α-helices (α3–α4), unlike previous FEN1 structures, which displayed unstable helical clamp regions. The structure of *Da*FEN1 may represent a 5′-flap structure-recognition state of a FEN1-family protein.

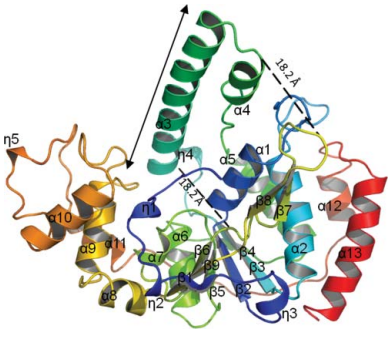

2. Methods and results

2.1. Structure determination

The expression, purification and crystallization of *Da*FEN1, as well as the preliminary X-ray crystallographic study, were performed as described by Mase *et al.* (2009). The *Da*FEN1 crystal diffracted X-rays to 2.00 Å resolution. The structure of *Da*FEN1 was determined by the molecular-replacement method. Molecular replacement was performed using the program *MOLREP* from the *CCP*4 suite (Collaborative Computational Project, Number 4, 1994) using the coordinates of FEN1 from *Pyrococcus horikoshii* (PDB code 1mc8; 57% sequence identity; Matsui *et al.*, 2002) as a search model. The initial structure was refined and rebuilt using the program *ARP*/*wARP* (Lamzin & Wilson, 1997). After automated model building and refinement, several cycles of manual model rebuilding, restrained refinement and TLS *B*-factor refinement were performed using the programs *REFMAC*5 (Murshudov *et al.*, 1997) from the *CCP*4 suite and *Coot* (Emsley & Cowtan, 2004). Water molecules were picked up from the $F_o - F_c$ map on the basis of peak height, distance and hydrogen-bonding criteria using the program *Coot*. The geometry of the final structure was evaluated with the program *RAMPAGE* (Lovell *et al.*, 2003). The coordinates of *Da*FEN1 were deposited in the Protein Data Bank (PDB) with accession code 3ory. A summary of the refinement statistics is provided in Table 1.

2.2. Structural analysis

Structural analysis was carried out using the following software programs: *DALI* (Holm *et al.*, 2008) was used to search for similar structures from the database, 3*D-Coffee* (O'Sullivan *et al.*, 2004) was used to align multiple sequences using structural information, *ESpript* (Gouet *et al.*, 1999) was used to prepare alignment figures, *MATRAS* (Kawabata, 2003) was used to calculate multiple structural alignment, *PyMOL* (http://www.pymol.org) was used to depict the structure and *DSSP* (Kabsch & Sander, 1983) was used to calculate secondary-structure assignments.

3. Results and discussion

3.1. Overall structure of *Da*FEN1

The crystal structure of *Da*FEN1 was determined at 2.00 Å resolution with *R*-factor and R_{free} values of 21.0% and 22.5%, respectively. The final model contained one *Da*FEN1 molecule and 101 water molecules in the asymmetric unit. Owing to the poor electron density, we could not build the coordinates of residues −10 to −4 and 340–353. In the Ramachandran plot, 98.8% of the residues were included in the favoured region and the remainder of the residues were in the allowed region. The refinement statistics of *Da*FEN1 are summarized in Table 1.

The structure of *Da*FEN1 is presented as a ribbon model in Fig. 1(*a*). *Da*FEN1 is composed of 13 α-helices (α1–α13) and nine β-strands (β1–β9), with topology η1-η2-β1-η3-β2-α1-α2-β3-η4-α3-α4-α5-β4-α6-β5-α7-β6-β7-β8-β9-α8-α9-α10-η5-α11-α12-α13, where η represents a 3_{10}-helix. The structure of *Da*FEN1 consists of a central six-stranded parallel β-sheet surrounded by α-helices, along with two additional small regions, which in FEN1-family proteins are called the 'helical clamp' (the region including α3 and α4 of *Da*FEN1) and the 'flexible loop' (the region including β7, the loop and β8 of *Da*FEN1), that extend out of the main body of the protein. The flat surface of the glycine-rich loop connecting the α9 and α10 helices has structural and sequence similarity to the DNA-binding helix–turn–helix (HTH) motif. In FEN1 proteins the HTH motif interacts with the phosphodiester backbone of the double-stranded DNA of the flap substrate (Hosfield *et al.*, 1998). In *Da*FEN1, 13 residues between the α9 and α10 helices form three turn structures, which may thus bind to substrate double-stranded DNA.

Table 1
Summary of data-collection and refinement statistics for *Da*FEN1.

Diffraction data collection	
Beamline	Photon Factory BL-5A
Space group	*P*321
Unit-cell parameters (Å)	$a = b = 103.76$, $c = 84.58$
Wavelength (Å)	1.00000
Resolution (Å)	50.0–2.00 (2.06–2.00)
No. of observations	389978 (26362)
No. of unique reflections	35852 (2607)
Data completeness (%)	99.8 (100)
Multiplicity	10.9 (10.1)
R_{merge}	0.037 (0.393)
$\langle I\rangle/\langle\sigma(I)\rangle$	41.73 (6.06)
Refinement	
R (%)	21.0
R_{free} (%)	22.5
No. of non-H atoms	
Protein	2701
Water	101
R.m.s. deviations	
Bond lengths (Å)	0.010
Bond angles (°)	1.119
Ramachandran plot (%)	
Favoured	98.8
Allowed	1.2
Disallowed	0

3.2. Comparison with other structures

A database search using the *DALI* server revealed that the overall structure of *Da*FEN1 is particularly similar to those of archaeal FEN1 proteins. Examples include the chain *A* structure of FEN1 from *P. horikoshii* (*Ph*FEN1; Matsui *et al.*, 2002; PDB entry 1mc8), which was used as a search model for structure determination by molecular replacement in the present study (*Z* score = 33.7, sequence identity = 59%, r.m.s.d. for 274 aligned C^{α} atoms = 2.0 Å), the chain *A* structure of FEN1 from *P. furiosus* (*Pf*FEN1; Hosfield *et al.*, 1998; PDB entry 1b43; *Z* score = 35.8, sequence identity = 60%, r.m.s.d. for 287 aligned C^{α} atoms = 2.2 Å) and the chain *A* structure of FEN1 from *Archaeoglobus fulgidus* (*Af*FEN1; Chapados *et al.*, 2004; PDB entry 1rxv; *Z* score = 34.4, sequence identity = 52%, r.m.s.d. for 301 aligned C^{α} atoms = 3.3 Å). In addition, the chain *X* structure of human FEN1 (hFEN1; Sakurai *et al.*, 2005; PDB entry 1ul1; *Z* score = 31.8, sequence identity = 38%, r.m.s.d. for 276 aligned C^{α} atoms = 2.6 Å) has a similar structure.

A multiple-sequence alignment shows a high degree of similarity in the active-site pocket residues between *Da*FEN1 and other FEN1-family proteins (Fig. 2). In particular, the sequence and structure of the Mg^{2+}-coordinating residues in the active-site pocket are highly conserved. In hFEN1 seven acidic residues (Asp34, Asp86, Glu158, Glu160, Asp179, Asp181 and Asp233) are assigned as active-site residues that tightly coordinate to two Mg^{2+} ions (Shen *et al.*, 1997). In *Da*FEN1 seven acidic residues (Asp31, Asp84, Glu156, Glu158, Asp177, Asp179 and Asp240) correspond to the acidic active-site residues of hFEN1 (Figs. 1*b* and 1*c*). These residues would form the active site of *Da*FEN1 and coordinate to the two Mg^{2+} ions which are necessary for enzymatic activity (Fig. 1*c*).

3.3. Additional residues in the N-terminal region

For structural analysis, we used a construct that has ten additional amino acids at its N-terminus (M^{-10}YIDQHNGVD^{-1}-*Da*FEN1) to obtain crystals that were suitable for X-ray diffraction measurements

(Mase *et al.*, 2009), based on the gene arrangement of *Da*FEN1 preceding the initiation methionine. In the crystal structure of *Da*FEN1 we built a structural model of the three amino-acid residues on the C-terminal side (GVD^{-1}; Figs. 1*d* and 1*e*). These three residues fill the active-site pocket to prevent substrates from accessing and coordinating to the Mg^{2+} ions; this prevention inhibits the enzymatic

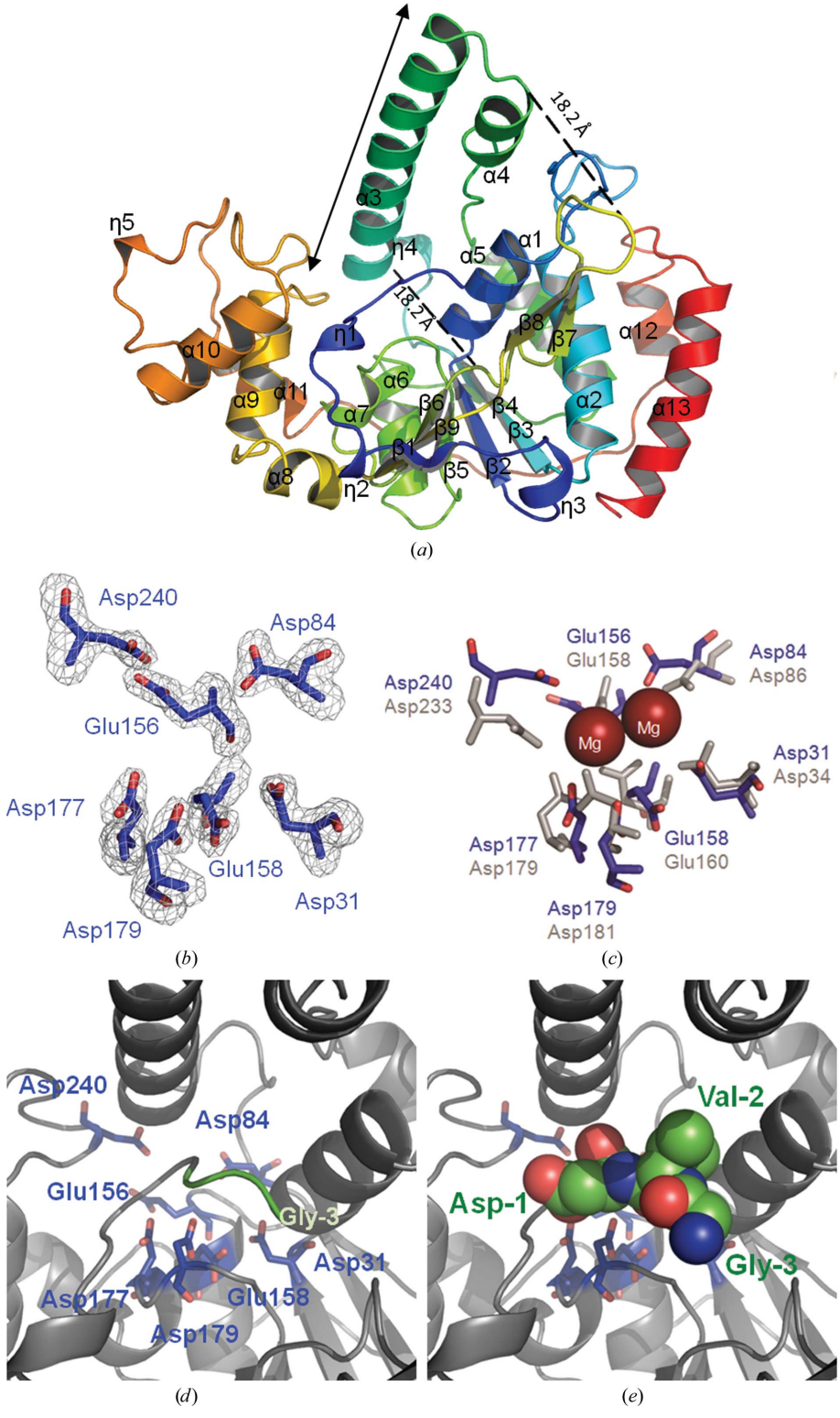

Figure 1
Structure of *Da*FEN1. (*a*) Ribbon diagram of *Da*FEN1. Colour-coding runs from blue at the N-terminal region to red at the C-terminal region. Secondary-structure assignments are labelled on the ribbon model. (*b*) σ_A-weighted $F_o - F_c$ OMIT map of the putative active site of *Da*FEN1. The map is contoured at 4σ. (*c*) Proposed Mg^{2+} positions in the *Da*FEN1 active site based on superposition of the *Da*FEN1 (blue) and hFEN1 (grey) active-site residues. Mg^{2+} ions are shown as red spheres. (*d*) Active-site structure of *Da*FEN1. Active-site acidic residues are shown as blue stick models. (*e*) Structure of the additional N-terminal residues of *Da*FEN1. These residues (Gly−3, Val−2 and Asp−1) are shown as sphere models.

activity of *Da*FEN1. The approximate distances between the C^{α} atoms of Asp−1 and Glu158 and between those of Val−2 and Asp31 were 13.7 and 13.9 Å, respectively. *Da*FEN1 with the ten additional N-terminal residues was found to have a lower enzymatic activity than wild-type *Da*FEN1 (data not shown). The observation that the N-terminal methionine residue was not observed in FEN1 proteins for which structures have been determined indicates that the decrease in enzymatic activity was not influenced by the positive charge of the N-terminus but simply by the existence of other residues. In addition, the sequence between Met−10 and Asp−1 of *Da*FEN1 is not conserved in FEN1-family proteins. According to this evidence, we presume that the starting methionine of *Da*FEN1 is Met1.

3.4. Unique structure of *Da*FEN1

A structural comparison of *Da*FEN1 with homologous proteins shows that the structure of *Da*FEN1 contains a unique helical clamp structure (Fig. 3*a*). *Da*FEN1 is the first FEN1 to show a well ordered helical clamp structure with a long α-helix (α3). Although this region has structural diversity among the FEN1-family proteins, the structure of the helical clamp region probably changes when it binds to the 5′-flap based on the results of mutation analysis (Matsui *et al.*, 2004; Storici *et al.*, 2002). One of the residues in the helical clamp region (Arg94) of *Pf*FEN1 has been predicted to bind the phosphate group at the cleavage site of substrate DNA after a substrate-induced conformational change in the helical clamp (Allawi *et al.*, 2003). The helical clamp region of *Da*FEN1 is mostly α-helical (the approximate length of the α3 helix is 34 Å) and differs from those of other FEN1 proteins, which are rich in loop structures or are disordered. Interestingly, Arg98 of *Da*FEN1, which corresponds to Arg94 of *Pf*FEN1, is located in the N-terminal part of the α3 helix near the putative active site (Fig. 3*a*).

*Da*FEN1 has an 'antiparallel ribbon' in the flexible-loop region which consists of antiparallel β-strands with a relatively long loop structure. A flexible loop containing such a ribbon has previously

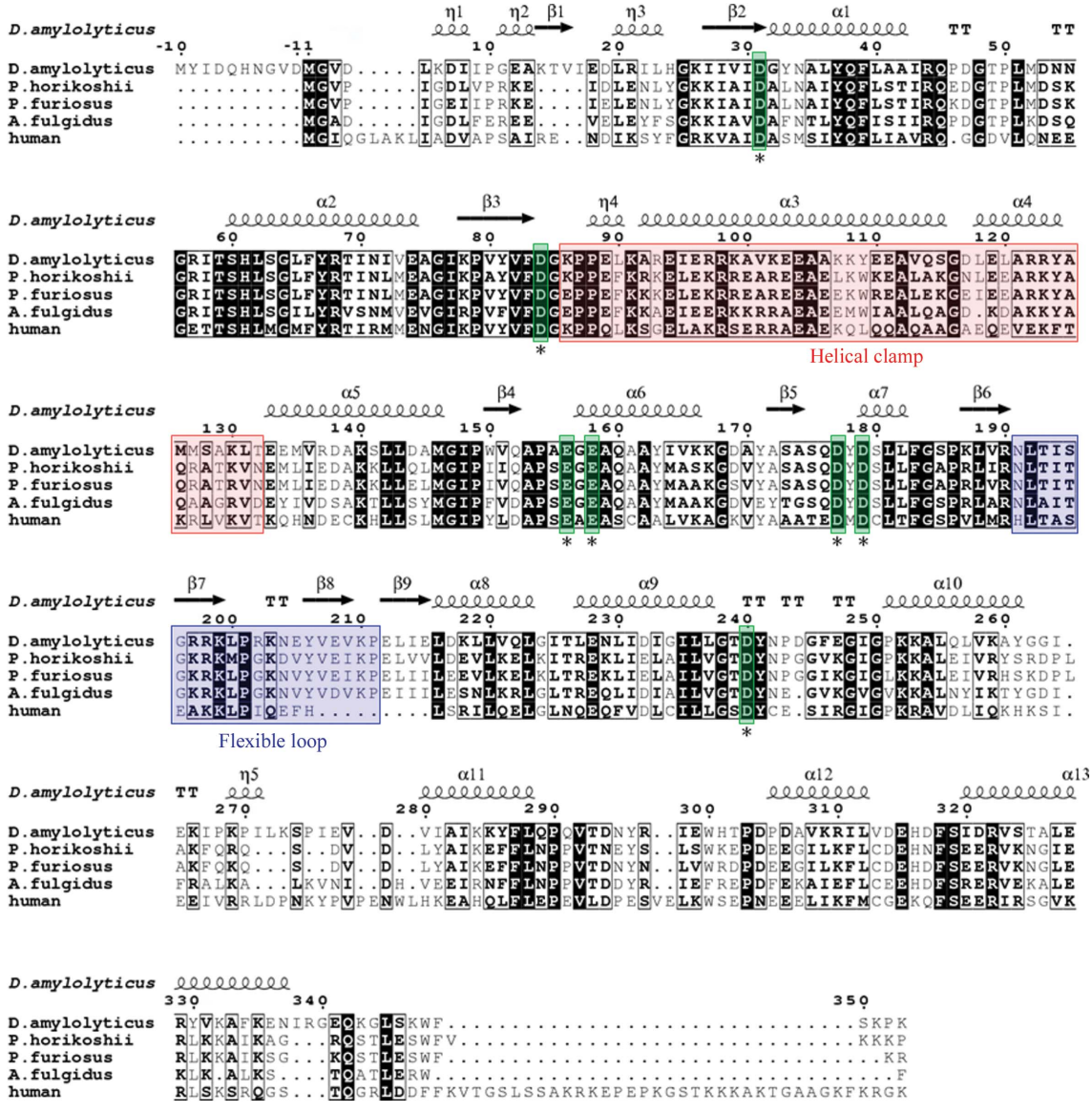

Figure 2
Amino-acid sequence alignment of *Da*FEN1 and other FEN1-family proteins [*P. horikoshii* FEN1 (PDB entry 1mc8), *P. furiosus* FEN1 (PDB entry 1b43), *A. fulgidus* FEN1 (PDB entry 1rxv) and human FEN1 (PDB entry 1ul1)]. The secondary-structure assignment of *Da*FEN1 is indicated by helices (α-helices and 3_{10}-helices) and arrows (β-strands). Highly conserved acidic residues in the active site are indicated by asterisks.

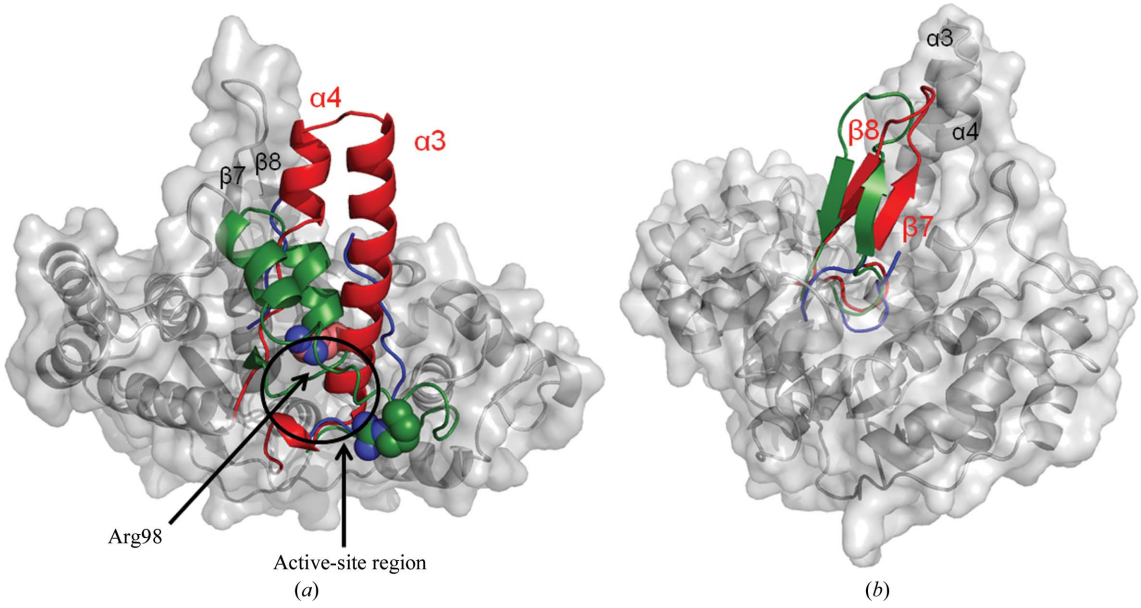

Figure 3
Comparison of *Da*FEN1 with other FEN1 proteins. (*a*) Comparison of the helical clamp structures of *Da*FEN1 (red) with *Pf*FEN1 and hFEN1 (green and blue, respectively). Arg98 of *Da*FEN1 and Arg94 of *Pf*FEN1 are shown as sphere models. (*b*) Comparison of the flexible-loop structure of *Da*FEN1 (red) with those of *Pf*FEN1 and hFEN1 (green and blue, respectively).

been reported in the structure of *Pf*FEN1 (Hosfield *et al.*, 1998) and this ribbon supports tighter binding to a flapped DNA than in eukaryotic FEN1 enzymes (Fig. 3*b*). However, the β-sheet is not present in *Ph*FEN1 (Matsui *et al.*, 2002). It has been reported that most eukaryotic FEN1 enzymes show a deletion of amino acids in this region and in the case of hFEN1 this deletion forms a shorter loop structure (Sakurai *et al.*, 2005).

In the structure of *Da*FEN1 the distances between the helical clamp and the flexible loop are estimated to be 18.2 and 18.2 Å between the C^{α} atoms of Glu94 and Asn191 and those of Glu119 and Lys203, respectively (Fig. 1*a*). The helical clamp and flexible loop form a hole that is sufficiently large to accommodate single-stranded DNA at the kinked position of the flap substrate. The results described in the present study may indicate that the helical clamp of FEN1 becomes α-helical as in the structure of *Da*FEN1 when the proteins bind and digest DNA with a flapped structure.

We are grateful to the staff members of beamline BL5A at the Photon Factory (Tsukuba, Japan; Proposal No. 2003S2-002). This work was supported in part by the National Project on Protein Structural and Functional Analyses and the Targeted Proteins Research Program (TPRP) of the Ministry of Education, Culture, Sports, Science and Technology, Japan.

References

Allawi, H., Kaiser, M., Onufriev, A., Ma, W., Brogaard, A., Case, D., Neri, B. & Lyamichev, V. (2003). *J. Mol. Biol.* **328**, 537–554.
Ceska, T., Sayers, J., Stier, G. & Suck, D. (1996). *Nature (London)*, **382**, 90–93.
Chapados, B., Hosfield, D., Han, S., Qiu, J., Yelent, B., Shen, B. & Tainer, J. (2004). *Cell*, **116**, 39–50.
Collaborative Computational Project, Number 4 (1994). *Acta Cryst.* D**50**, 760–763.
Devos, J., Tomanicek, S., Jones, C., Nossal, N. & Mueser, T. (2007). *J. Biol. Chem.* **282**, 31713–31724.
Emsley, P. & Cowtan, K. (2004). *Acta Cryst.* D**60**, 2126–2132.
Freudenreich, C., Kantrow, S. & Zakian, V. (1998). *Science*, **279**, 853–856.
Gouet, P., Courcelle, E., Stuart, D. & Métoz, F. (1999). *Bioinformatics*, **15**, 305–308.
Harrington, J. & Lieber, M. (1994). *EMBO J.* **13**, 1235–1246.
Holm, L., Kääriäinen, S., Rosenström, P. & Schenkel, A. (2008). *Bioinformatics*, **24**, 2780–2781.
Hosfield, D., Mol, C., Shen, B. & Tainer, J. (1998). *Cell*, **95**, 135–146.
Hwang, K., Baek, K., Kim, H. & Cho, Y. (1998). *Nature Struct. Biol.* **5**, 707–713.
Kabsch, W. & Sander, C. (1983). *Biopolymers*, **22**, 2577–2637.
Kaiser, M., Lyamicheva, N., Ma, W., Miller, C., Neri, B., Fors, L. & Lyamichev, V. (1999). *J. Biol. Chem.* **274**, 21387–21394.
Kawabata, T. (2003). *Nucleic Acids Res.* **31**, 3367–3369.
Kil, Y., Baitin, D., Masui, R., Bonch-Osmolovskaya, E., Kuramitsu, S. & Lanzov, V. (2000). *J. Bacteriol.* **182**, 130–134.
Kim, Y., Eom, S., Wang, J., Lee, D., Suh, S. & Steitz, T. (1995). *Nature (London)*, **376**, 612–616.
Lamzin, V. & Wilson, K. (1997). *Methods Enzymol.* **277**, 269–305.
Lovell, S., Davis, I., Arendall, W. III, de Bakker, P., Word, J., Prisant, M., Richardson, J. & Richardson, D. (2003). *Proteins*, **50**, 437–450.
Mase, T., Kubota, K., Miyazono, K., Kawarabayasi, Y. & Tanokura, M. (2009). *Acta Cryst.* F**65**, 923–925.
Matsui, E., Abe, J., Yokoyama, H. & Matsui, I. (2004). *J. Biol. Chem.* **279**, 16687–16696.
Matsui, E., Musti, K., Abe, J., Yamasaki, K., Matsui, I. & Harata, K. (2002). *J. Biol. Chem.* **277**, 37840–37847.
Mueser, T., Nossal, N. & Hyde, C. (1996). *Cell*, **85**, 1101–1112.
Murante, R., Huang, L., Turchi, J. & Bambara, R. (1994). *J. Biol. Chem.* **269**, 1191–1196.
Murante, R., Rust, L. & Bambara, R. (1995). *J. Biol. Chem.* **270**, 30377–30383.
Murshudov, G. N., Vagin, A. A. & Dodson, E. J. (1997). *Acta Cryst.* D**53**, 240–255.
O'Sullivan, O., Suhre, K., Abergel, C., Higgins, D. G. & Notredame, C. (2004). *J. Mol. Biol.* **340**, 385–395.
Sakurai, S., Kitano, K., Yamaguchi, H., Hamada, K., Okada, K., Fukuda, K., Uchida, M., Ohtsuka, E., Morioka, H. & Hakoshima, T. (2005). *EMBO J.* **24**, 683–693.
Schweitzer, J. & Livingston, D. (1998). *Hum. Mol. Genet.* **7**, 69–74.
Shen, B., Nolan, J., Sklar, L. & Park, M. (1997). *Nucleic Acids Res.* **25**, 3332–3338.
Storici, F., Henneke, G., Ferrari, E., Gordenin, D., Hübscher, U. & Resnick, M. (2002). *EMBO J.* **21**, 5930–5942.
Tishkoff, D., Filosi, N., Gaida, G. & Kolodner, R. (1997). *Cell*, **88**, 253–263.